



## RECENT STUDIES ON INERTER-EQUIPPED ROCKING STRUCTURES

R. Thiers-Moggia<sup>(1)</sup>, C. Málaga-Chuquitaype<sup>(2)</sup>

<sup>(1)</sup> PhD Researcher, Imperial College London, London, United Kingdom, [r.thiers16@imperial.ac.uk](mailto:r.thiers16@imperial.ac.uk)

<sup>(2)</sup> Senior Lecturer, Imperial College London, London, United Kingdom, [c.malaga@imperial.ac.uk](mailto:c.malaga@imperial.ac.uk)

### **Abstract**

When subjected to base motion, a variety of structures, such as museum artefacts, historical buildings, bridge piers and post-tensioned walls, might uplift and set into rocking motion. Although this mechanism can efficiently limit the internal forces at their base, the possibility of overturning or experiencing increased lateral demands can affect the functionality of rocking structures. Nevertheless, suitable seismic control strategies are presently limited and concentrate on either preventing the rocking motion altogether, a solution that can induce undesirable stress concentrations; or installing highly intrusive structural control devices like active and passive dampers that may lead to impractical retrofitting schemes. Moreover, in those cases where rocking is used to enable self-centring mechanisms in building structures, uplift and the subsequent contact action will inevitably induce high acceleration demands that the addition of pre-stressing may exacerbate. Recently, the use of supplemental rotational inertia devices to control the seismic response of rocking structures has been proposed by the authors. This new strategy employs inerters, which are mechanical devices that develop resisting forces proportional to the relative acceleration between their terminals and can be combined with clutches to ensure they act only in opposition to the motion. This paper presents an overview of recent studies concerning the fundamental dynamics and practical application of inerters on rocking structures. Firstly, the fundamental dynamic behaviour of the system is examined considering a free-standing rigid block model. It is demonstrated that the inclusion of the inerter effectively reduces the frequency parameter of the block, resulting in lower seismic demands and enhanced stability due to the well-known size effects of the rocking behaviour. The simplified single-degree-of-freedom rocking model is gradually extended in order to incorporate the effects of post-tensioned tendons, structural flexibility and higher modes on the response and to highlight issues related to the practical implementation of the inerter system. Overall, the analyses conducted under both coherent pulses and real ground motion records show that inerter-equipped rocking structures experience reduced seismic demands and lower probabilities of exceeding limit states associated with structural and non-structural damage.

*Keywords: Rocking structures; inerter; clutch; seismic control; damage assessment*



## 1. Introduction

Traditional seismic design methodologies aim to prevent structural collapse by ensuring a minimum level of strength and deformation capacity in the lateral-load-resisting system of a building. Initially developed in the 50's and 60's [1], these strength and ductility considerations remain today as the basis for current seismic design provisions. Although, in general, this philosophy has succeeded in preventing structural collapse and protecting lives, recent earthquakes have revealed that in many cases the extent of damage can make repairs infeasible, highlighting the mismatch between social expectations and the actual seismic performance of civil structures. Over the last decades, the alternative approach of allowing structures to uplift and rock has been gaining popularity as a strategy to control structural damage during earthquakes. Although the survival of ancient Greek temples has been attributed to this unintended response mechanism [2], it was not until 1963 that George Housner elucidated a size-frequency scale effect that explained the counter-intuitive seismic stability of tall, slender rocking structures [3]. Since then, his simplified analytical model has been used to analyse the seismic response of rocking structures and has served as the basis for the development of low-damage post-tensioned rocking buildings [4]. While experimental studies have demonstrated that these systems can efficiently control structural damage, modern performance-based methodologies have also highlighted the importance of assessing non-structural and contents damage, which can significantly affect the total losses and downtime costs after a seismic event.

Rocking motion is not constrained to new building applications, but its relevant to a large variety of structures, such as museum artefacts and historical buildings. In all these cases, the possibility of overturning or experiencing increased lateral deformations and accelerations have motivated engineers to explore dynamic control strategies with unintended negative consequences like fixing the structures at their base to prevent uplifting. In fact, investigations on control strategies suitable to rocking bodies have been limited and have mainly concentrated on the protection of museum artefacts and non-structural equipment [5,6]. Early strategies were based on simple measures, such as lowering the centre of mass or anchoring the object to a fixed support. These solution can induce undesirable stress concentrations and changes the dynamic response of rocking structures potentially making them more vulnerable. For example, Makris and Zhang [7] first analysed the stability of rigid blocks tied down with brittle and ductile restrainers, concluding that anchorages can have an adverse effect on the stability of the structure. Aiming to address this issue, Ceravolo et al. [6] proposed the use of semi-active anchorages with variable stiffness and compared different strategies for their implementation. Their analyses showed that feedback control strategies based on the block's angular position and velocity significantly improved its dynamic response and stability. Importantly, the controlled cases were generally more stable than both the freestanding blocks and structures anchored with passive restraint systems such as elastic-brittle plates and viscous dampers. Other studies have proposed the use of viscous dampers [8,9], pendulum mass dampers hinged at the top of the rocking body [10], seismic isolation [11], and more recently the use of external resonators as a means to control the peak seismic rotational demands of rocking monumental structures [12]. In many cases, the proposed alternatives are usually only effective for a limited range of frequencies or structural dimensions. This highlights the need for more robust non-intrusive solutions suitable for uplifting rocking bodies.

This paper deals with the use of inerters to control the dynamic response of rocking structures, large and small. The inerter, a mechanical device that develop resisting forces proportional to the relative acceleration between its terminals, can be combined with clutches to ensure it acts only in opposition to the motion. To this end, this paper presents an overview of recent studies concerning the fundamental dynamics and practical application of inerters to a variety of structures that uplift and rock. Firstly, the fundamental dynamic behaviour of the system is examined considering a free-standing rigid block model. This simplified single-degree-of-freedom model is gradually extended to incorporate the effects of post-tensioned tendons, structural flexibility, and higher modes on the response and to highlight issues related to the practical implementation of the system. Overall, the analyses presented demonstrate that the inclusion of the inerter results in lower seismic demands and enhanced stability of rocking structures.



## 2. Supplemental inertial devices: inerters

An efficient seismic control strategy that has been gaining popularity over the last years involves the use of supplemental rotational inertia. Based on this concept, Arakaki et al. [13] first developed a damper formed of a cylindrical mass rotating inside a chamber filled with a viscous fluid in the late 90's. This mechanical arrangement was rediscovered in the west under the name of inerter [14] and applied to vehicle suspensions systems. The inerter develops a resisting force in proportion to accelerations. Accordingly, in a force-current/velocity-voltage analogy, the inerter is the mechanical analogue of the capacitor and its constant of proportionality is called inertance (with units of mass) [14]. Typical inerter realizations employ rack-and-pinion [14,15] or ball-screw mechanisms [16,17] to transform the relative displacement between the terminals into a rotation in a flywheel. Papageorgiou et al. [18, 19] tested both configurations, showing that rotation-amplification mechanisms can significantly increase the inertance of the device while keeping the associated gravitational mass minimum.

Recent studies have highlighted the potential advantages of employing inerters to control the seismic response of civil structures. Hwang et al. [20] investigated the vibration control effect of a rotational inertia damper combined with a toggle bracing on a fixed-base single degree-of-freedom structure. A similar evaluation was conducted by Ikago et al. [16], who included a flywheel to increase the inertial effects of the device. Makris and Kampas [15] studied the case of an elastic frame connected to rack-pinion-flywheel system and demonstrated that inerters are particularly effective in reducing peak displacements for long-period structures. Importantly, they noted that this happens at the expense of transferring considerable forces to the support of the flywheels. Their study also explored the use of a clutch to ensure the inerter only resists the structural motion without inducing additional deformations, a strategy that was further investigated experimentally and numerically by Málaga-Chuquitaype et al. [21]. The proposed arrangement was able to further reduce the structural displacements, whereas mixed results were obtained for the transferred forces. Chen et al. [22], on the other hand, studied the influence of supplemental rotational inertia on the natural frequencies of multi degree-of-freedom systems.

Several applications of the inerter have been proposed within the context of enhancing the performance of tuned mass dampers. Ikago et al. [16] proposed a Tuned Viscous Mass Damper (TVMD) consisting of a viscous inerter connected in series to a linear spring and used it to control the response of a simplified 10-storey structure. In this case, the TVMDs were equally distributed along the height of the building, following the recommendations given by Takewaki et al. [23]. Lazar et al. [24] developed a Tuned Inerter Damper (TID) and presented expressions to obtain the optimal parameters of the device based on H1 optimization criteria. The main advantages of these configurations included an improved reduction of peak deformations and a wider suppression band. The mass-amplification effect of the inerter has also been harnessed to improve the performance of vibration barriers [12,25] and to reduce the displacement demands of base isolation systems [26]. Importantly, all these previous studies have focused on the seismic control of fixed-based structures.

## 3. Inerter-equipped free-standing rigid rocking blocks

Although the free vibration frequency of a rocking block is not constant, its dynamic properties can be characterized by the frequency parameter  $p$ , which represents the in-plane pendulum frequency of the same block dangling from its pivot point [27]. For a rectangular block like the one depicted in Fig. 1,  $p = \sqrt{3g/4R}$ . Assuming that no sliding or bouncing occurs during impact, the planar rocking motion of the structure under a ground motion ( $\ddot{u}_g$ ) can be described by means of Housner's model [3] as follows:

$$\ddot{\theta} = -p^2 \left( \sin(\alpha \operatorname{sgn}(\theta) - \theta) + \frac{\ddot{u}_g}{g} \cos(\alpha \operatorname{sgn}(\theta) - \theta) \right) \quad (1)$$

Thiers-Moggia and Málaga-Chuquitaype [28] demonstrated that when an inerter is added to the rocking system, the question of motion becomes:

$$\ddot{\theta} = -p_\sigma^2 \left( \sin(\alpha \operatorname{sgn}(\theta) - \theta) + \frac{\ddot{u}_g}{g} \cos(\alpha \operatorname{sgn}(\theta) - \theta) \right) \quad (2)$$



where

$$p_{\sigma} = \sqrt{\frac{3g}{R(4+3\sigma \cos^2(\alpha \operatorname{sgn}(\theta) - \theta))}} \quad (3)$$

In this equation,  $\sigma = m_r/m$  is the apparent mass ratio and the other geometric parameters are defined in Fig. 1. Eqs. 1 to 3 show that the inclusion of the inerter has an effect equivalent to reducing the frequency parameter,  $p$ , of the block. This effect depends on the magnitude of the rotation  $\theta$ , reaching a maximum when  $\theta = \alpha$  and becoming less significant for higher rotations. In general, the reduction of the frequency parameter should result in lower seismic demands due to the size effect of rocking behaviour [3]. This principle dictates that among two blocks of the same slenderness  $\alpha$ , the one with the lower frequency parameter,  $p$  (larger in size), is more stable and therefore has lower levels of structural demands. It is important to note that for a given rectangular block, the frequency parameter,  $p$ , depends only on the size,  $R$ , and therefore cannot be modified without altering its geometry. Consequently, the use of supplemental rotational inertia devices configures a practical alternative to modify the dynamic response and reduce seismic demands in rocking structures. Importantly, the clutched pair of inerters proposed by Makris and Kampas [15] can be easily incorporated into the above mathematical formulation. To this end, the effects of the apparent mass of the inerter are re-evaluated after each integration step [28].

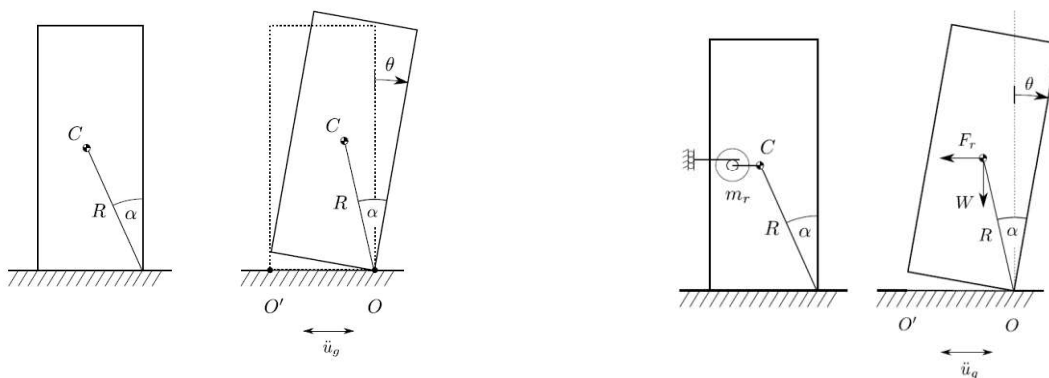


Fig. 1 – Rigid rocking block under a horizontal ground excitation. Free-standing rocking block (left) and Rocking block with an inerter of rotational mass  $m_r$  (right)

It has also been demonstrated by Thiers-Moggia and Málaga-Chuquitaype, that the inclusion of the inerter does not affect significantly the similarity laws governing the motion of rocking bodies. However, in the case of clutched systems, the inclusion of the inerter-clutch device adds an additional source of non-linearity to the equation of motion, and the response becomes non or less self-similar. This is an important outcome that was found to affect more the later stage of the response.

The rocking response of a rigid block can result in one of two outcomes: (a) safe rocking, where the block survives the ground motion and the energy is dissipated through successive impacts at the base until the motion stops; and (b) overturning, where the equation of motion leads to an arbitrarily large rotation value and the block topples. Overturning is usually studied by means of overturning plots like the ones presented in Fig. 2. These plots show the regions in the frequency-amplitude acceleration space that result in safe rocking or overturning of the block. The area above the upper curves in the graphs of Fig. 2 represent overturning without impact (Region 1), whereas the areas enclosed by the lower curves correspond to overturning taking place after impact at the base [27] (Region 2). The remaining regions of the plot are associated with safe rocking (Region 3).

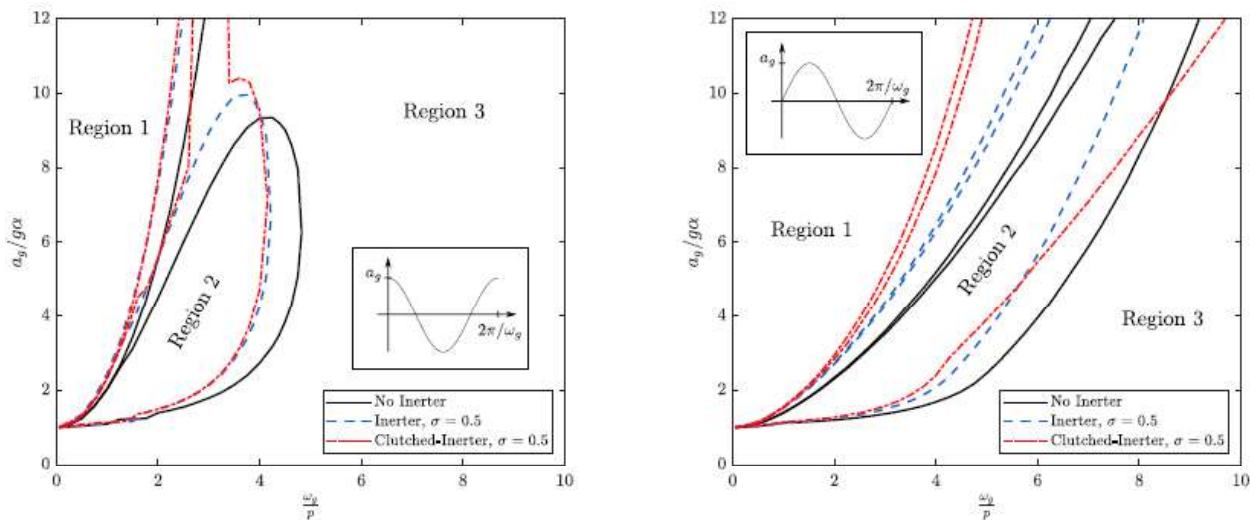


Fig. 2 – Overturning plots of a slender ( $\alpha = 10^\circ$ ) rocking-block-inerter systems subjected to cosinusoidal pulses (left) and sinusoidal pulses (right)

It can be appreciated from Fig. 2 that, in general, the inclusion of the inerter reduces the areas of overturning (Regions 1 and 2) and translates them to the lower frequency region. This frequency shift, which is otherwise beneficial, is particularly relevant for the case of overturning after impact (Region 2), as certain blocks that would rock safely without the inerter, may overturn when the protective device is incorporated. Similar trends have been observed for the non-slender blocks [28]. The effect of the inerter on the overturning response is considerably less significant for smaller objects. Therefore, the use of a higher mass ratio,  $\sigma$ , will be necessary to further improve the stability of such blocks under single pulse excitations.

The advantages brought about using the inerter were also verified for real ground motions. To this end, Fig. 3 presents overturning fragility functions obtained from response-history analyses with a set of 202 real pulse-like ground motion records obtained from the Pacific Earthquake Engineering Research Center (PEER) database. Records from 21 earthquakes with magnitudes  $M_w$  ranging from 5.4 to 7.9 were considered. The probabilities of overturning depicted in Fig. 3 are conditioned on the dimensionless intensity measure  $IM = pPGV/g \tan \alpha$  in attention to previous studies that have shown that rocking response is particularly sensitive to the velocity and acceleration characteristics of the ground motion. The fragility functions depicted in Fig. 3 show a significant improvement in the overturning performance of the block equipped with inerters. The estimated mean IM for the unprotected block is  $\hat{\mu} = 0.93$ , whereas this parameter increases to  $\hat{\mu} = 1$  and  $\hat{\mu} = 1.16$  when a single inerter and a pair of clutched inerters with  $\sigma = 0.5$  are employed. The overturning probabilities are further reduced if higher inertances are employed (i.e.  $\sigma = 1$ ) where reductions in mean probabilities of toppling of around 50% are experienced for the clutched inerters configuration. These reduction levels are maintained for probabilities of exceedance of 10% as appreciated from Fig. 3. These results are in line with the demand reductions observed previously and allow to conclude that the use inerters is an efficient mechanism to reduce maximum rotations and improve the overturning response of rocking blocks under pulse-like ground motions.

#### 4. Inerter-equipped post-tensioned rocking structures

The previous section has examined the response of rocking structures equipped with supplemental rotational inertia devices using a simplified rigid-block formulation. While this model captures reasonably well the behaviour of free-standing bodies, such as non-structural equipment and museum artefacts, it does not represent the response of post-tensioned building structures. These aspects will be analysed in this section.

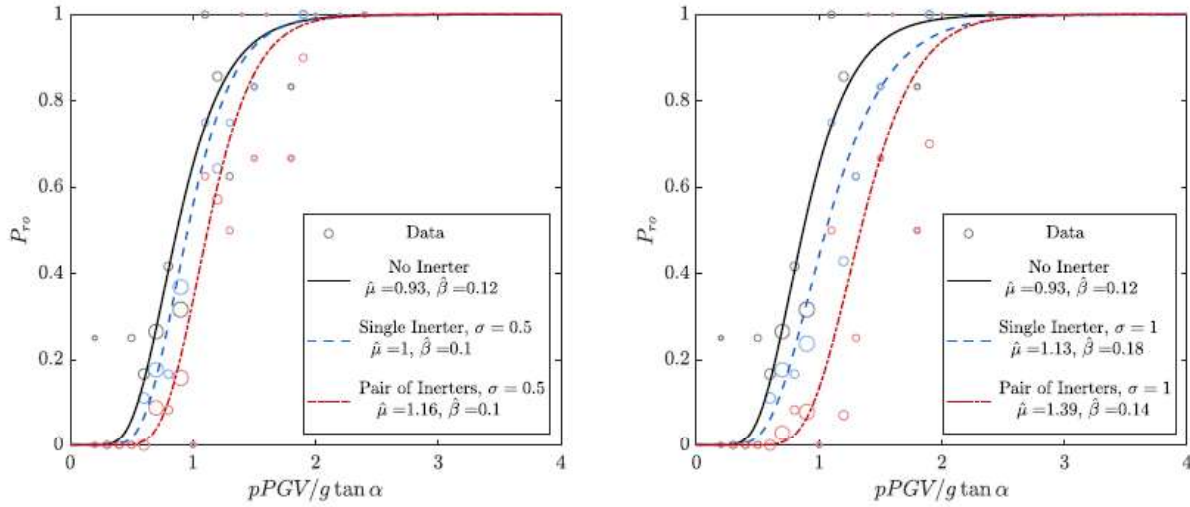


Fig. 3 – Comparison of overturning probabilities for a slender rigid block of  $\alpha = 10^\circ$  and  $R = 1$  [m] for mass ratios of  $\sigma = 0.5$  (left) and  $\sigma = 1.0$  (right)

The equation describing the rocking response of post-tensioned walls is:

$$\ddot{\theta} = -p_{w,\sigma}^2 \left( \sin(\alpha \operatorname{sgn}(\theta) - \theta) + m_{ratio} \frac{\ddot{u}_g}{g} \cos(\alpha \operatorname{sgn}(\theta) - \theta) + \sin \alpha \left( \frac{EA}{W} \tan \alpha \sin \theta + \operatorname{sgn}(\theta) \frac{P_o}{W} \sqrt{\frac{1 + \cos \theta}{2}} \right) \right) \quad (4)$$

where  $m_{ratio}$  is the ratio of the seismic mass to the gravitational mass associated with the gravity load transferred to the wall ( $W$ ) [29],  $E$  is the elastic modulus of the tendon material,  $A$  is the axial area of the tendon,  $P_o$  is the initial post-tensioning, and  $p_{w,\sigma}$  is a new frequency parameters defined as [29]:

$$p_{w,\sigma} = \sqrt{\frac{g}{m_{ratio} R (1 + \sigma \cos^2(\alpha \operatorname{sgn}(\theta) - \theta))}} \quad (5)$$

Importantly, previous investigations [28, 30] have demonstrated that the effect of the inerter on impact is very small when slender structures are considered. Therefore, the coefficient of restitution can be assumed to be a constant and independent parameter of the structural system.

Fig. 4 presents the results of a cloud analysis considering the same earthquake database used above. Results are presented in terms of rotation and rotational acceleration fragilities for post-tensioned structures with and without inerters. The uniform duration,  $t_{uni}$ , which corresponds to the sum of the time intervals during which the ground acceleration exceeds the limit to cause uplifting, was selected as the intensity measure, as recommended by Dimitrakopoulos and Giouvanidis [31]. A power law is assumed to relate the median estimated demand and the earthquake intensity measure  $IM$ .

In general, the structure equipped with inerter devices shows significantly smaller seismic demands for the whole  $IM$  range. Mean reductions of around 50% are observed in both peak rotations and peak accelerations. These conclusions are consistent with observations made for single pulse excitations [29]. The fragility functions depicted in Fig. 4 demonstrate the significant improvement in the performance of post-tensioned rocking structures brought about by the inerter. In terms of rotations, the estimated median  $IM$  associated with the selected drift limit state is  $\sim t_{uni} = 0.5$  [s] for the unprotected structure, whereas this parameter increases to  $\sim t_{uni} = 0.74$  [s] when the inerter is introduced. Moreover, the response enhancement becomes more important for higher probabilities of exceedance. Similar trends are observed in the case of peak floor

accelerations, with an even greater increase (nearly four-fold) in the median IM. On the other hand, smaller variations were obtained on the logarithmic standard deviation. This supports the conclusion that inerters configure a practical alternative to improve the dynamic response and boost the overall seismic performance of post-tensioned rocking structures.

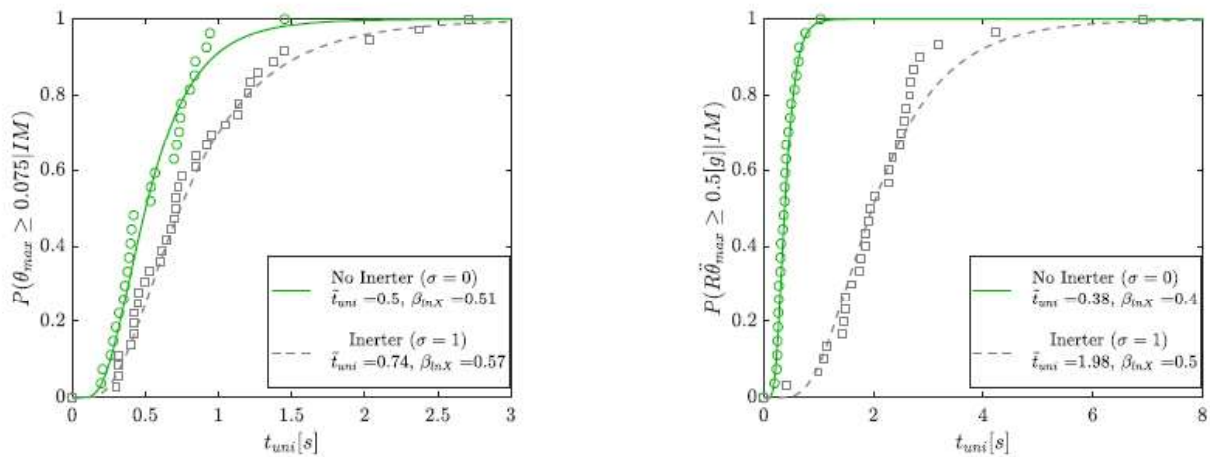


Fig. 4 – Fragility functions for post-tensioned rocking walls with and without inerters for a rotation limit of  $\theta_{max} = 0.75\%$  (left) and an acceleration limit of  $R\theta_{max} = 0.5 [g]$

## 5. Inerter-equipped flexible rocking structures

In some practical applications, the degree of flexibility of the rocking body cannot be neglected. Moreover, some of the underlying assumptions of the analytical models used to study rigid bodies imply that the structures are slender, and therefore more likely to deform during the rocking motion. These instances highlight the need for a rigorous assessment of the dynamics of flexible uplifting structures equipped with inerters and a detailed quantification of the effects of flexibility on the efficiency of the system. These aspects were studied by Thiers-Moggia and Málaga-Chuquitaype [32] and are summarized here. In their study, Thiers-Moggia and Málaga-Chuquitaype proposed an original analytical model based on the expressions developed by Oliveto et al. [33] by considering the effects of grounded supplemental rotational inertia devices. Additionally, two previously proposed impact formulations [34, 35] were implemented and compared. The possibility of using inerters to control the elastic deformation at uplifted resonance of flexible rocking structures was also examined [32].

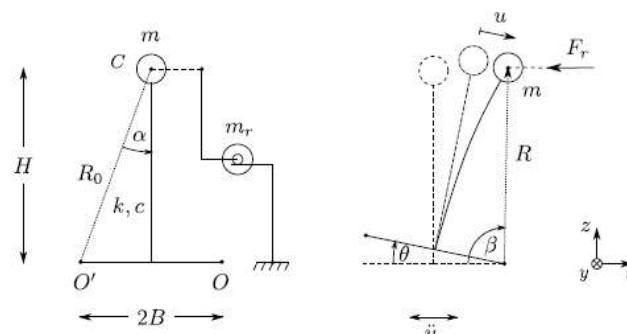


Fig. 5 – Idealized analytical model of a flexible rocking structure connected to an inerter

The dynamic response of the structure shown in Fig. 5 can be divided into two phases: i) a full contact phase, where there is no base rotation; and ii) a rocking phase, where the base uplifts and the system rocks and oscillates simultaneously. An elastic structure whose motion starts from rest will respond initially in the full contact phase until uplift ensues. After base uplifting, the structure will transition into a rocking motion and experience both rotational and translational deformations. During the full contact phase, the initial dynamic



response of an inerter-equipped flexible rocking structure can be described by the following equation of motion:

$$\ddot{u} + \frac{2\xi\omega_n}{(1+\sigma)}\dot{u} + \frac{\omega_n^2}{(1+\sigma)}u = -\frac{\ddot{u}_g}{(1+\sigma)} \quad (6)$$

where  $\omega_n$  and  $\xi$  are the natural frequency and damping ratio of the fixed base flexible oscillator. While the equations that describe the motion of the uplifted flexible rocking structure are [30,32]:

$$\ddot{R} + \sigma((\ddot{R} - R\dot{\beta}^2) \cos^2 \beta - (2\dot{R}\dot{\beta} + R\ddot{\beta}) \cos \beta \sin \beta) = \omega_n^2 R \left( \frac{B}{\sqrt{R^2 - H^2}} - 1 \right) - \frac{2\xi\omega_n R^2 \dot{R}}{R^2 - H^2} + R\dot{\beta}^2 \pm \ddot{u}_g \cos \beta \mp g \sin \beta \quad (7)$$

$$\ddot{\beta} - \frac{\sigma}{R} \left( (\ddot{R} - R\dot{\beta}^2) \cos \beta \sin \beta - (2\dot{R}\dot{\beta} + R\ddot{\beta}) \sin^2 \beta \right) = -\frac{2\dot{R}\dot{\beta}}{R} \mp \frac{g}{R} \cos \beta \mp \frac{\ddot{u}_g}{R} \sin \beta \quad (8)$$

The effect of the inerter on the elastic deformation of the oscillator,  $u$ , is highly influenced by the occurrence or not of the rocking motion. For very flexible oscillators (small  $\omega_n/p$ ) the uplift condition is not reached, and the response approximates that of fixed-base inerter-equipped single-degree-of-freedom systems. However, the onset of rocking, clearly identifiable as a crest in the elastic deformation response of Fig. 6, significantly alters the behaviour of the system. Once rocking motion is triggered, the effect of the inerter on the elastic deformation of the oscillator is very limited, and no significant gains are observed as the clutch is introduced although the benefits of the clutch become more relevant as the oscillator's stiffness increases. Nevertheless, the overall effect of the inerter on total drifts is still appreciable after uplift due to the important rotational reductions brought about by the supplemental inertia.

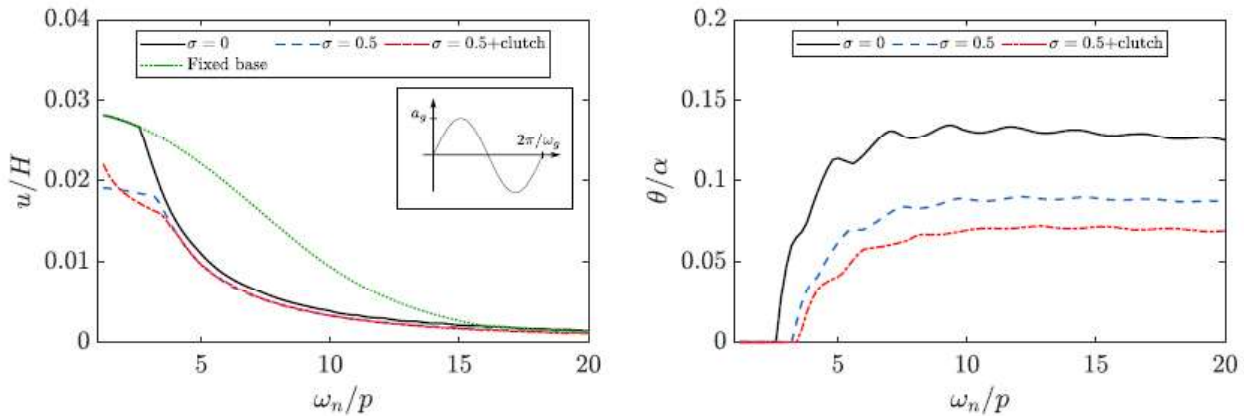


Fig. 6 – Effect of flexibility on the response of structures with  $\xi = 0.02$ , with and without inerters, subjected to sine pulses of  $\omega_g/p = 8$  and  $a_g = 1.5g \tan \alpha$ . Elastic deformations (left) and base rotation (right)

The global stability of flexible rocking structures is studied with reference to the overturning plots presented in Fig. 7. These results are consistent with the trends previously observed for rigid rocking bodies [28]. In both cases the inclusion of the inerter reduces the areas of overturning (Regions 1 and 2) and translates them to the lower frequency region. This frequency shift, which is otherwise beneficial, is particularly relevant for the case of overturning after impact (Region 2), as certain structures that would rock safely without the inerter, may overturn when the protective device is incorporated. The introduction of the clutch, on the other hand, further shifts the overturning regions and expands the overturning after impact area (Region 2) to higher acceleration magnitudes, a potential drawback that was also identified for rigid bodies [28]. Nevertheless, this



adverse effect occurs in a frequency-acceleration region of limited practical relevance. Of particular interest in stability analyses are smaller structures, which are known to be more vulnerable to overturning during strong ground motions [3]. In these cases, the effect of the inerter becomes less significant, and higher levels of inertances may be required to considerably improve the stability of the oscillator. In this regard, the actual mass of the inerter can be reduced in several orders of magnitude by using amplification mechanisms such as ball-screws or gear systems [21]. Alternatively, the incorporation of a clutch can also enhance the performance of the inerter device in smaller unstable structures.

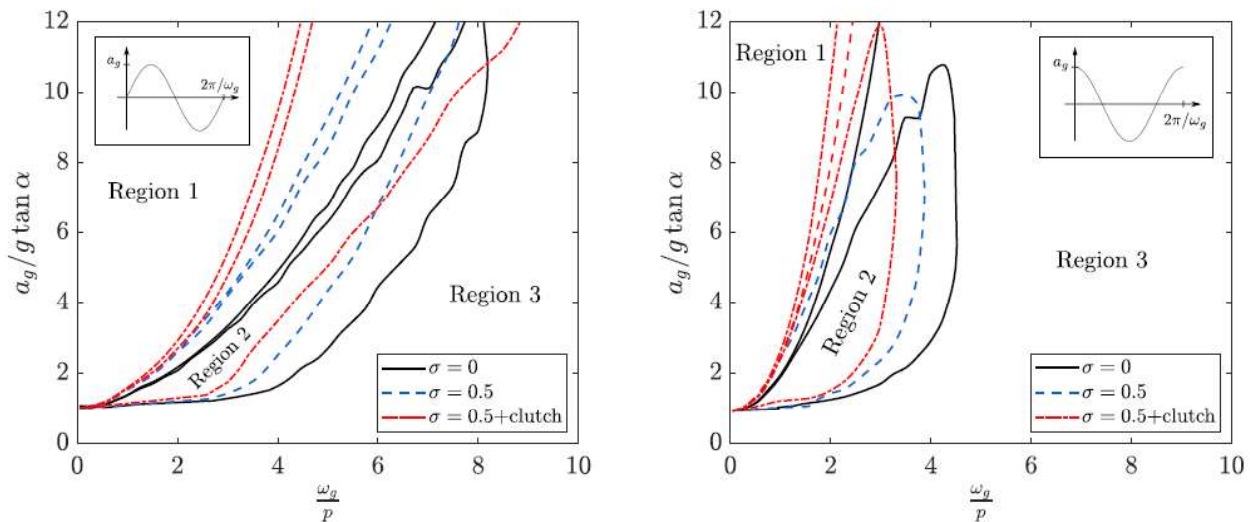


Fig. 7 – Overturning response of flexible rocking structures with  $\omega_n/p = 10$ ,  $\xi = 0.02$  and  $\alpha = 0.2$  under sinusoidal pulses (left) and cosinusoidal pulses (right)

## 6. Inerter-equipped self-centring rocking buildings

The important advantages of coupling intertters with rocking structures identified above have been applied to the seismic design and assessment of multi-storey post-tensioned rocking walled buildings by Thiers-Moggia and Málaga-Chuquitaype [36]. To this end, numerical models were built in OpenSees [37]. A schematic view of the multi-mass flexible numerical model employed is presented in Fig. 8. The buildings analysed have dimensions of 12x10 meters in plan, and have an inter-storey height of 3 meters. The structural plan consists of a frame in the transverse direction supporting gravity loads, and four post-tensioned walls providing lateral load resistance in each direction. Structures of 3, 6 and 9 storeys using Cross Laminated Timber (CLT) walls were designed according to Direct Displacement Based Design principles [38].

Both bare and inerter-equipped structures were examined and subjected to the suite of 202 ground motion records described previously. The Cloud to IDA procedure proposed by Miano et al. [39] was used for the estimation of the structural fragilities. This methodology employs the critical demand to capacity ratio (DCR) as the performance variable, thus facilitating the identification of intensity values at the onset of a desired limit state. In this way, IDA curves can be obtained for a selected group of ground motion records with a minimum amount of scaling, which is known to be particularly problematic when pulse-like records are considered. Fig. 9 summarises the results in terms of drift and acceleration fragilities for the 3-storey building case.

The fragility functions shown in Fig 9 demonstrate that, in general, the inerter equipped structures have lower probabilities of reaching the defined limit states for any given IM value. In particular, the mean spectral acceleration,  $S_a(T_1)$ , required to exceed the assumed drift limit grows considerably when the intertters are incorporated, although this effect becomes less significant as the structures become taller. Moreover, the



incorporation of inerters tends to increase the variability of the lateral deformation response. The combination of these effects explains the behaviour observed in the drift fragility plots, where a better response control is obtained for larger probabilities of exceedance, and small differences are observed under lower seismic intensities.

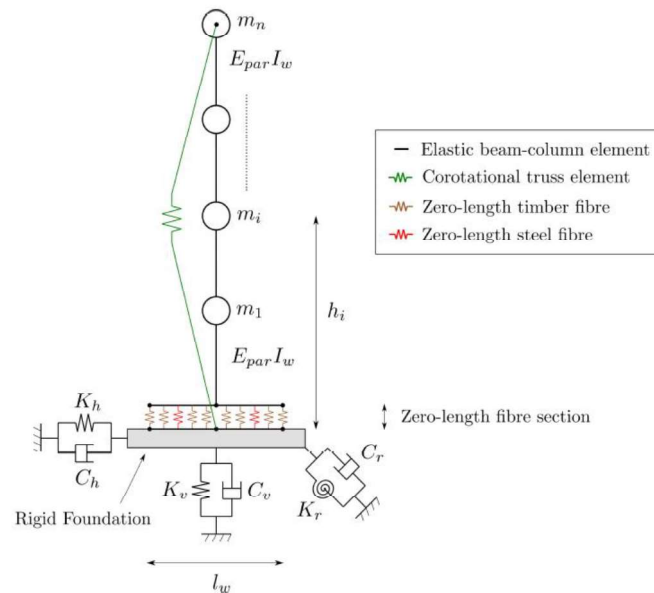


Fig. 8 – Schematic diagram of the numerical model of the rocking building with post-tensioned walls [36]

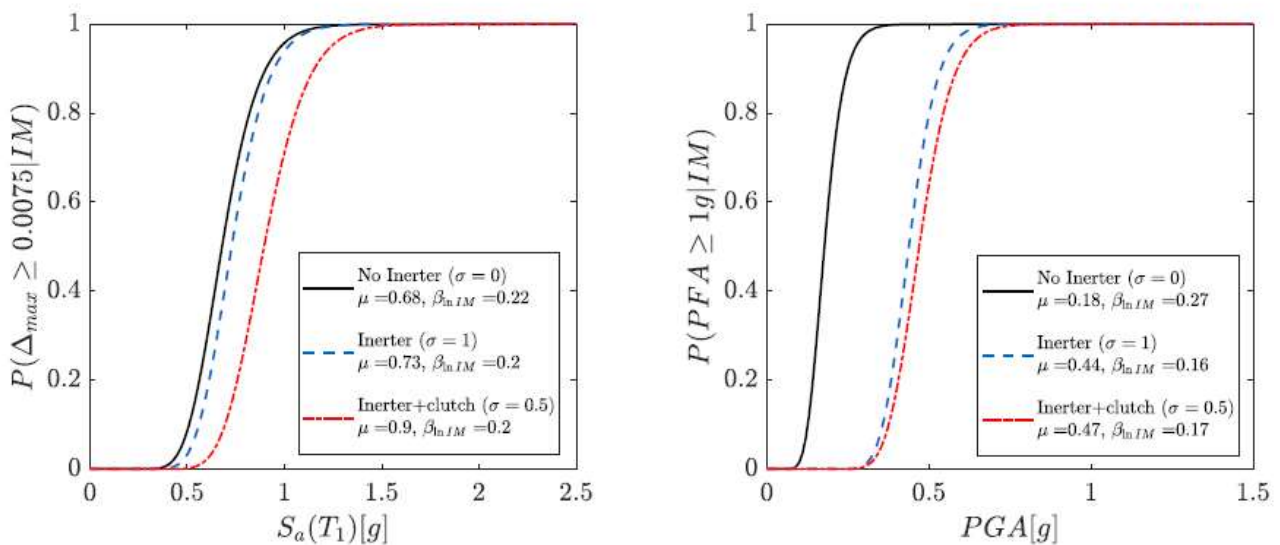


Fig. 9 – Structural fragilities for the defined limit states of 0.75% inter-storey drift (left) and 1g peak floor acceleration (right) for a 3 storey rocking timber building

## 7. Conclusions

This paper has examined the possibility of employing inerters to improve the seismic performance of rocking structures. Several recent studies have been summarized that provide a comprehensive and rigorous examination of the dynamic response of rocking structures equipped with supplemental rotational inertia devices. The results presented have highlighted the ability of the inerter to improve the seismic performance of various types of rocking structures ranging from rigid free-standing bodies, to flexible uplifting structures



and post-tensioned buildings. In a context where most seismic control strategies for rocking structures have adapted measures previously developed for fixed-base buildings, the innovative solution offered by inerters is worth noting. Through a combination of analytical, numerical and design studies the efficiency of the proposed strategy to control not only peak deformations but also peak accelerations has been established. Besides, evaluations conducted within a performance-based framework have confirmed that rocking structures coupled with inerters experience lower probabilities of exceeding limit states associated with both structural and non-structural damage.

## 6. References

- [1] Baker J (1956), *The Steel Skeleton*, Vol. 2. Cambridge University Press.
- [2] Makris N (2014), A half-century of rocking isolation. *Earthquakes and Structures*,7(6): 1187-1221.
- [3] Housner G (1963), The behavior of inverted pendulum structures during earthquakes. *Bulletin of the Seismological Society of America*, 53:403-417.
- [4] Priestley MJN (1919), An overview of PRESSS research program. *PCI Journal*, 36(4).
- [5] Calio I, Marletta M (2003), Passive control of the seismic rocking response of art objects. *Engineering Structures*, 25(8): 1009-1018.
- [6] Ceravolo R, Pecorelli M, and Fragonara LZ (2016), Semi-active control of the rocking motion of monolithic art objects. *Journal of Sound and Vibration*, 374:1-16.
- [7] Makris N, Zhang J (1999), Rocking response and overturning of anchored equipment under seismic excitation, *Report Pacific Earthquake Engineering Research Centre*, Berkeley, US.
- [8] Dimitrakopoulos E, DeJong M (2012), Overturning of retrofitted rocking structures under pulse-type excitations. *Journal of Engineering Mechanics*, 138(8): 963-972.
- [9] Makris N, Aghagholizadeh M (2019), Effect of supplemental hysteretic and viscous damping on rocking response of free-standing columns. *Journal of Engineering Mechanics*, 145(5): 04019028.
- [10] deLeo A, Simoneschi G, Fabrizio C, DiEgidio A (2016), On the use of a pendulum as mass damper to control the rocking motion of a rigid block with fixed characteristics. *Meccanica*, 5: 2727-2740.
- [11] Vassiliou M, Makris N (2012), Analysis of the rocking response of rigid blocks standing free on a seismically isolated base. *Earthquake Engineering & Structural Dynamics*, vol. 41: 177-196.
- [12] Pan X, Málaga-Chuquitaype C (2020), Seismic control of rocking structures via external resonators. *Earthquake Engineering & Structural Dynamics*, 49(12):1180-1196.
- [13] Arakaki T, Kuroda H, Arima F, Inoue Y, Baba K (1999), Development of seismic devices applied to ball screw. Part 1: Basic performance of test RD-series, *AIJ Journal of Technology and Design*, 8:239-244.
- [14] Smith M (2002), Synthesis of mechanical networks: The Inerter. *IEEE Transactions on Automatic Control*, 47(10):1648-1662.
- [15] Makris N, Kampas G (2016), Seismic protection of structures with supplemental rotational inertia. *Journal of Engineering Mechanics*, 142:1-11.
- [16] Ikago K, Saito K, Inoue N (2012). Seismic control of single-degree-of-freedom structure using tuned viscous damper. *Earthquake Engineering & Structural Dynamics*, 41(3):436-474.
- [17] Nakamura Y, Fukukita A, Tamura K, Yamazaki I, Matsuoka T, Hiramoto K, Sunakoda K (2014), Seismic response control using electromagnetic inertial mass dampers. *Earthquake Engineering & Structural Dynamics*, 43 (4): 507-527.
- [18] Papageorgiou C, Smith M (2005), Laboratory experimental testing of inerters. *Proc. 44th IEEE Conference on Decision and Control*, IEEE, New York, 3351-3356.
- [19] Papageorgiou C, Houghton N, Smith M (2008), Experimental testing and analysis of inerter devices. *Journal of Dynamic Systems, Measurement, and Control*, 131, 12.



- [20] Hwang J, Kim J, Kim Y (2007), Rotational inertia dampers with toggle bracing for vibration control of a building structure. *Engineering Structures*, 29: 1201-1208.
- [21] Málaga-Chuquitaype C, Menendez-Vicente C, Thiers-Moggia R (2019), Experimental and numerical assessment of the seismic response of steel structures with clutched inerters. *Soil Dynamics and Earthquake Engineering*, 121:200-211.
- [22] Chen M, Hu Y, Huang L, Chen G (2014), Influence of inerter on natural frequencies of vibration systems. *Journal of Sound and Vibration*, 333(7): 1874-1887.
- [23] Takewaki I, Murakami S, Yoshitomi S, and Tsuji M (2012), Fundamental mechanism of earthquake response reduction in building structures with inertial dampers. *Structural Control and Health Monitoring*, (19): 590-608.
- [24] Lazar I, Neild S, Wagg D (2014), Using an inerter-based device for structural vibration suppression. *Earthquake Engineering & Structural Dynamics*, 43 (8): 1129-1147.
- [25] Cacciola P, Tombari A, Giaralis A (2020), An inerter-equipped vibrating barrier for non-invasive motion control of seismically excited structures. *Structural Control and Health Monitoring*, 27(3): 2474.
- [26] DeDomenico D, Ricciard G (2018), An enhanced base isolation system equipped with optimal tuned mass damper inerter (tmdi). *Earthquake Engineering & Structural Dynamics*, 47(5): 1169-1192.
- [27] Makris N, Vassiliou M (2012), Planar rocking response and stability analysis of an array of free-standing columns capped with a freely supported rigid beam. *Earthquake Engineering & Structural Dynamics*, 42 (3): 431-449.
- [28] Thiers-Moggia R, Málaga-Chuquitaype C (2019), Seismic protection of rocking structures with inerters. *Earthquake Engineering & Structural Dynamics*. 48(5):528-47.
- [29] Thiers-Moggia R, Málaga-Chuquitaype C (2020), Dynamic response of post-tensioned rocking structures with inerters. *International Journal of Mechanical Sciences*, 187:105927.
- [30] Thiers-Moggia R (2020), Seismic control of rocking structures using inerters. *PhD Thesis*, Imperial College London, UK.
- [31] Dimitrakopoulos E, Giouvanidis A (2018), Rocking amplification and strong-motion duration. *Earthquake Engineering & Structural Dynamics*, 1-22.
- [32] Thiers-Moggia R, Málaga-Chuquitaype C (2020). Seismic control of flexible rocking structures using inerters. *Earthquake Engineering & Structural Dynamics*, 49(14):1519-38.
- [33] Oliveto G, Calio I, Greco A (2003), Large displacement behaviour of a structural model with foundation uplift under impulsive and earthquake excitations, *Earthquake Engineering & Structural Dynamics*, 32(3): 369-393.
- [34] Chopra A, SCS Y (1985), Simplified earthquake analysis of structures with foundation uplift. *Journal of Structural Engineering*, 111(4): 906-930.
- [35] Vassiliou M, Truniger R, Stojadinovic B (2015), An analytical model of a deformable cantilever structure rocking on a rigid surface: development and verification. *Earthquake Engineering & Structural Dynamics*, 44 (15): 2775-2794.
- [36] Thiers-Moggia R, Málaga-Chuquitaype C (2021). Performance-based seismic design and assessment of rocking timber buildings coupled with inerters. *Submitted*.
- [37] McKenna F, Scott MH, Fenves GL (2010), Nonlinear finite-element analysis software architecture using object composition. *Journal of Computing in Civil Engineering*, 24(1):95-107.
- [38] Priestley MJN, Calvi GM, Kowalsky M (2007), *Displacement-Based Seismic Design of Structures*. IUSS PRESS, Pavia, Italy.
- [39] Miano A, Jalayer F, Ebrahimian H, Prota A (2018), Cloud to IDA: Efficient fragility assessment with limited scaling. *Earthquake Engineering & Structural Dynamics*, 47(5). 1124-1147.